ELSEVIER

Fuel Processing Technology 72 (2001) 163–183

FUEL PROCESSING TECHNOLOGY

www.elsevier.com/locate/fuproc

Effect of bed materials and additives on the sintering of coal ashes relevant to agglomeration in fluidized bed combustion

C. Tangsathitkulchai [a,*], M. Tangsathitkulchai [b]

[a] *School of Chemical Engineering, Institute of Engineering, Suranaree University of Technology, Nakhon Ratchasima 30000, Thailand*

[b] *School of Chemistry, Institute of Science, Suranaree University of Technology, Nakhon Ratchasima 30000, Thailand*

Received 1 August 2000; received in revised form 1 March 2001; accepted 1 March 2001

Abstract

Agglomeration propensity of Thai low-rank coal ashes was determined by measuring the compressive strength of sintered ash pellets over the temperature range of fluidized bed combustion. Physical and chemical changes of the sintered products were ascertained from scanning electron microscope-energy dispersive X-ray detection (SEM-EDX) and X-ray diffractometry (XRD). A clear difference existed in the strength–temperature relationship between these ashes. This difference was attributed to the role and relative amounts of clays and anhydrite components that form the low temperature melting eutectics. The bed materials (sand, CaO, $CaCO_3$, and $CaSO_4$) and additives (gibbsite and andalusite) when combined with the ashes caused a strength reduction due to the inert dilution effect that prevented the interaction of anhydrite and clays. To comprehend the mechanism of sintering and bed agglomeration more clearly, modified ashes which produced extra amount of amorphous silicate materials were prepared and tested. The bed materials and additives, when sintered with these modified ashes, gave reduction of pellet strength by varying extents based on three possible mechanisms namely, a pure inert effect, an inert/reaction effect and an inert/adsorption effect, with gibbsite being the most effective. Of the four test ashes, Lanna ash was the only ash that exhibited almost no strength development under all conditions, due principally to its very low clays content and relatively stable forms of mineralogical compositions.

Keywords: Sintering; Coal ash; Bed agglomeration; Bed materials

* Corresponding author. Fax: +66-44-224-220.
E-mail address: chaiyot@ccs.sut.ac.th (C. Tangsathitkulchai).

0378-3820/01/$ - see front matter
PII: S0378-3820(01)00191-6

1. Introduction

Fluidized bed combustion is considered to be a suitable technology for burning a wide range of fuels. A particular advantage is its ability to maintain combustion temperatures (800–900 °C) below ash fusion point and this also leads to lower nitrogen oxides emission. In addition, the introduction of limestone sorbent offers opportunity for in-bed capture of sulfur dioxide generated from the combustion process. Therefore, fluidized bed combustion has been increasingly used by industries and utilities as an effective and environmentally acceptable means for producing steam for process heat and electricity generation. In a fluidized bed combustor, the suspension of bed particles can consist of particles of combusting coal, coal ash, fluidizing sand, limestone, calcium oxide and calcium sulfate. The proper fluidization of these particles needs to be maintained in order to stabilize the furnace operation. Under certain conditions, however, agglomeration of bed particles can occur. In the most serious case, rapid sintering can lead to severe agglomerate formation, causing defluidization and subsequent shut down of the combustor [1–3].

Brown et al. [4] suggested that agglomeration occurred as a result of the interaction between the sticky ash with other bed particles. Sintering and secondary reactions appear to occur after the agglomerates have formed and tend to strengthen the agglomerates. The problem of growth in the size of bed material particles during fluidized bed combustion of lignite containing high levels of sodium and sulfur has been reported by Manzoori [1]. He reported that the ash component was transferred from the burning char particles to the bed particles, coating them with sticky material and thus facilitating the formation and sintering of agglomerates. Steenari et al. [5] examined agglomerated bed materials and deposits from fluidized bed combustors. They found that the agglomerates consisted of predominant amorphous phase and other crystalline phases. The amorphous phase probably formed from silicate–alkali interaction and the crystalline phases were $CaSO_4$, $CaCO_3$, SiO_2 and Fe_2O_3. Bhattacharya [3] studied combustion of high sodium and high sulfur low rank coals and found the minor crystalline phase to be sulfates of calcium, magnesium and sodium. According to these previous works, the formation of bed agglomeration consists of initial adhesion between sticky ash particles and bed materials followed by further ash-bed particle interaction. This initial sticking and sintering of ash-bed particles is controlled by the low-melting phases formed from ash constituents. Several investigators [6–8] have therefore studied control methods for mitigating the agglomeration problem mainly by suppressing the formation of these low-melting eutectics. Linjewile and Manzoori [6] investigated the effects of four additives (dolomite, gibbsite, kaolinite and sillimanite-rich clay, and kaolinite and quartz-rich clay) on bed material–ash adhesion as compared to the test without additives during circulating fluidized bed combustion of low-rank coals. The coating on spent bed material recovered from the tests without additive was enriched in sodium and sulfur compounds. The role of additives in controlling ash agglomeration has been found to be either a chemical effect or a physical dilution effect, depending on the interaction between each additive and the ash particles. Gibbsite, kaolinite and sillimanite-rich clay were found to be the most effective additives. Vuthaluru and Zhang [7] and Vulthaluru

et al. [8] further studied the use of alternative bed materials (bauxite and sillimanite) and coal pretreatment (water washing, acid washing and aluminium pretreatment). Aluminium enrichment in ash was found to suppress the formation of low-melting eutectics when alternative bed materials and aluminium pretreated coal were used. Acid washing did not improve the operation of the bed burning test coals. In the case of water washing, the effective agglomeration control was due to the reduced level of sodium, which modified the ash properties.

Although it is common practice to investigate the bed agglomeration problem by performing tests on a small-scale fluidized bed combustor, a laboratory ash sintering test is useful in acquiring preliminary trend and prediction information as to the level of bed agglomeration and deposition problems in fluidized bed combustors [9,10]. The sintering behaviour of different coal ashes varies widely depending on ash chemistry and other factors such as ash particle shape, size and distribution of sizes, furnace temperature and atmosphere that influence the course of ash sintering process [11–13]. In a fluidized bed combustor, in addition to physical parameters such as fluidization characteristics and mixing, bed materials such as fluidizing sand (SiO_2), sorbents (CaO, $CaCO_3$) and sorbent product ($CaSO_4$) may incorporate into the agglomerates and further complicate the ash sintering behaviour.

There are some good reviews of available laboratory techniques for ash sintering predictions [14–17]. Several investigators [9,18–24] have used the ash pellet compressive strength measurement developed by Barnhart and Williams [25] to determine the sintering behaviour of coal ashes. The compressive strength of sintered ash pellets was measured as a function of sintering temperature followed by the evaluation of physical and chemical changes of the sintered ash particles. The present investigator previously used this method for studying the sintering behaviour of various fly ashes as related to deposit formation in pulverized coal combustion [19]. It was concluded that glass material in the as-received fly ashes was the component that contributed most to the formation of strong deposits. However, when the glass material associated with the alkalis, alkaline earths, and iron in the as-received fly ash these glass components underwent devitrification to form crystalline phases. As a result of glass material removal, the rate of sintering was reduced and sintered strength was low. Past information on the sintering behaviour of coal ashes has been mostly generated for pulverized coal combustion and thus the information obtained may not be applicable to the sintering behaviour of ash under fluidized bed combustion. In addition, the interaction between ash components and bed particles, and additives that are incorporated into the agglomerates is not well understood.

The purpose of this study was to investigate the bed agglomeration tendency of coal ashes by following their sintering behaviour as well as the role and mechanism of bed materials and additives. In this work, the compressive strength measurement was used to follow the extent of ash sintering under the operating temperatures of a fluidized bed combustor. It has been reported that the bed agglomeration involves the association of amorphous sticky ash with bed materials [3,5]. To enable a more precise study of bed agglomeration, this amorphous phase matrix was purposely created within the sintered ash particles by mixing the amorphous silica with the original ash and sintering experiments performed. This modified ash, when mixed with bed materials and additives

particles, would allow a closer study as to the interacting role of these materials during the sintering and agglomeration process.

2. Experimental

The four sample coals used are low-rank coals from the Maemoh seam, Banpu seam, Chiengmuan seam and Lanna seam, all of which located in the northern area of Thailand and supplied by the Electricity Generating Authority of Thailand (EGAT). The coal samples were crushed and ground to pass minus 60 mesh (250 μm) screen size, and the ashes were prepared from these sized coals by using the standard ASTM ashing procedure [26]. Ash compositions as percent oxide were determined using an X-ray fluorescence spectrometer (XRF).

A pellet was formed from 0.12 g of ash sample, mixed with a drop of water and pressed in a cylindrical die to give a pellet of 0.5 cm in diameter and 0.5 cm in height, giving a bulk density of 1200 kg m^{-3}. The presence of small amount of added water in the pellet was considered to have negligible cementation effect caused by the pozzolanic reaction between alumina or silica and calcium hydroxide presenting in the ash. This was further confirmed by the fact that the prepared pellet had no detectable strength as measured by a compressive strength tester (Wykeham Farrance, UK). Eight pellets were placed in an alumina crucible and subsequently heated in an electrical tube furnace (Carbolite, England) to the desired temperature at the rate of 10 °C/min in air, and held at that temperature for 4 h. The furnace temperature was measured by a Pt/Pt–10%Rh thermocouple and was controlled by a microprocessor control system. Sintering temperatures in the range 800–1050 °C were studied. At the completion of each test, the sintered pellets were cooled to room temperature inside the furnace. The dimensions of the cold pellets were measured and the compressive strength of the six pellets determined by the compressive strength tester to obtain the average value. It should be noted that in measuring pellet strength, the cylindrical pellet was compressed along its long axis to obtain the true compressive strength. The remaining two pellets were kept for further analyses. The sintering of coal ash mixed with bed materials and additives was studied by adding each of the following materials, sand (SiO_2), sorbents (CaO, $CaCO_3$), sorbent product ($CaSO_4$), andalusite (Al_2SiO_5) and gibbsite ($Al(OH)_3$) at 15 wt.% into the ashes. Andalusite is a naturally occurring mineral, called refractory oxide and is another crystalline form of sillimanite. It is richer in Al_2O_3 and is generally used to increase the refractoriness of silicate composition in ceramic industries. Gibbsite dehydrates to amorphous Al_2O_3 at 300 °C. These two additives when added to coal ash were expected to behave as bed agglomeration inhibitors. The modified ash was prepared by mixing 15 wt.% amorphous silica into the pure ash and sintered it at various temperatures. All the added materials were sized to pass a 60 mesh (250 μm) screen.

The compressive strength tests were supplemented with physical and chemical analyses of selected sintered products. The SEM-EDX (JEOL JSM-6400, Oxford 6209) and XRD analyses (Philips X-ray diffractometer, X' Pert PW3710) were performed to identify the mineralogical phase changes of the sintered ash product. For XRD analysis a

step scan of 0.02° per minute was used to ensure sufficient time to discriminate low-intensity peaks from the background.

3. Results and discussion

3.1. Particle size distributions and ash characteristics

Size distributions of ash samples, bed materials and additives were measured with a laser-diffraction particle analyzer (Model-Mastersizer S, Malvern Instruments, UK) and are summarized in Table 1. It can be seen that size distributions of the four ash samples are comparable, with the mass mean diameters being 40.2, 32.1, 41.1 and 31.4 μm for Maemoh, Banpu, Chiengmuan and Lanna ASTM ashes, respectively. In general, bed materials and additives particles possess finer size distributions than those of ash particles, with gibbsite having the finest size distribution. From the consideration of all size distribution data, it can be observed that more than 50% of particles are in the sub-sieve size range (−35 μm) and approximately 30% of particles being smaller than 10 μm. With this fineness of particle sizes, and hence a relatively large surface area of particles, the ability of additives and bed materials to chemically react with the reactive ash constituents is possible.

Proximate analyses of the raw coals are tabulated in Table 2. The elemental compositions (as %oxide) of the four test ashes as determined by XRF analysis are

Table 1
Particle size distributions of ash samples, bed materials and additives

Particle size (μm)	Cumulative weight percent smaller than size								
	Ash samples				Bed materials			Additives	
	Maemoh	Banpu	Chiengmuan	Lanna	$CaCO_3$	$CaSO_4$	Sand	Andalusite	Gibbsite
200	100.00	100.00	100.00	100.00	100.00	100.00	100.00	100.00	100.00
150	98.97	99.18	98.80	99.62	100.00	99.87	99.20	96.14	100.00
112	95.23	97.36	94.45	98.22	100.00	97.14	98.34	87.63	100.00
84	88.10	93.30	86.90	94.95	99.86	90.40	96.47	75.47	100.00
62	77.70	86.32	76.48	88.56	95.77	78.98	92.77	62.61	99.98
46	65.52	76.87	64.73	78.73	86.30	64.34	87.05	51.94	99.10
35	53.96	66.39	53.74	66.60	71.77	50.10	79.93	43.78	97.62
26	43.81	56.63	44.08	54.45	54.68	38.69	72.29	37.69	90.27
19	35.39	48.05	35.95	43.28	39.20	30.38	64.66	32.82	76.53
15	28.51	40.72	29.15	33.77	27.00	24.72	57.22	28.53	58.46
11	22.85	34.42	23.44	26.18	18.83	20.78	50.13	24.58	42.01
8	18.18	28.86	18.66	20.39	14.14	17.74	43.57	21.02	29.69
6	14.40	23.84	14.78	16.13	11.68	15.03	37.61	17.94	21.73
4.5	11.42	19.30	11.71	13.05	10.37	12.79	32.18	15.31	17.16
3.3	9.13	15.30	9.35	10.82	9.50	10.74	27.09	13.07	14.63
2.5	7.14	11.96	7.55	9.20	8.79	9.05	22.24	11.12	13.15
Mass mean diameter (μm)	40.2	32.1	41.1	31.4	26.5	39.8	22.0	52.8	14.5

Table 2
Proximate analysis of test coals

Percentage (dry basis)	Maemoh	Banpu	Chiengmuan	Lanna
Volatile matter	48.2	34.3	42.1	34.0
Ash	30.1	35.6	30.2	36.1
Fixed carbon	21.7	30.1	27.7	29.9

summarized in Table 3. Banpu and Chiengmuan ashes have higher acidic oxide (Al_2O_3, SiO_2) contents but less basic oxide (CaO, Na_2O) and SO_3 than Maemoh ash and Lanna ash. Lanna ash contains the lowest amounts of Al_2O_3 and SiO_2, and the highest amounts of Fe_2O_3, MgO and CaO. XRF results are in agreement with the phase compositions analyzed by XRD. That is, the results from XRD of Maemoh ash and Lanna ash (Tables 4a and d) indicate that anhydrite ($CaSO_4$) is the major crystalline phase with quartz (SiO_2) being the minor phase. Chiengmuan ash and Banpu ash show different results, with quartz being the major phase and anhydrite the minor phase (Tables 4b and c).

3.2. Sintering of pure coal ashes

Sintering behaviour of the four test ashes is depicted in Fig. 1 in terms of strength variation with temperature over the range 800–1050 °C. For temperatures up to 1000 °C, the strength tended to increase linearly with increasing temperature, except Lanna ash which showed relatively low and relatively unchanged value of strength over this temperature range. For this temperature range, the following order of strength was observed: Maemoh > Chiengmuan > Banpu > Lanna, with maximum strength of about 12 MPa being observed at 1000 °C for Maemoh ash and Chiengmuan ash.

In this study, sinter point (T_{SINT}) is defined as the temperature at which the ash pellet starts to develop a measurable strength. As shown in Fig. 1, this temperature was approximately determined by extrapolating the lower straight-line portion of strength–

Table 3
Oxide analysis of ASTM ash samples by X-ray fluorescence method

%Oxide	Maemoh	Banpu	Chiengmuan	Lanna
SiO_2	32.9	58.8	49.2	18.0
Al_2O_3	18.9	29.2	23.1	8.1
TiO_2	0.4	0.6	0.6	0.2
Fe_2O_3	11.4	4.4	7.3	13.8
MgO	2.4	1.2	2.3	4.2
CaO	15.6	1.4	7.2	23.7
MnO	0.16	0.001	0.04	0.10
K_2O	2.4	2.3	2.3	1.1
Na_2O	0.83	0.20	0.07	1.1
P_2O_5	0.15	0.03	0.05	0.10
SO_3	14.1	2.1	6.3	29.5

Table 4
XRD analysis of test ashes

Ash condition	Major crystalline phases	Minor crystalline phases
(a) Maemoh ash		
Unheated	anhydrite [$CaSO_4$]	quartz [SiO_2], hematite [Fe_2O_3]
900 °C	anhydrite [$CaSO_4$]	quartz [SiO_2], hematite [Fe_2O_3], amorphous phase
1050 °C	anorthite [$CaAl_2Si_2O_8$]	diopside [$CaMg(SiO_3)_2$], hematite [Fe_2O_3], cristobalite [SiO_2], trunscottite [$Ca_2Si_4O_9$], quartz [SiO_2], amorphous phase
(b) Chiengmuan ash		
Unheated	quartz [SiO_2]	anhydrite [$CaSO_4$], hematite [Fe_2O_3]
900 °C	quartz [SiO_2]	anhydrite [$CaSO_4$], hematite [Fe_2O_3]
1050 °C	quartz [SiO_2]	anhydrite [$CaSO_4$], albite [$NaAlSi_3O_8$], hematite [Fe_2O_3], amorphous phase
(c) Banpu ash		
Unheated	quartz [SiO_2]	anhydrite [$CaSO_4$], hematite [Fe_2O_3]
900 °C	quartz [SiO_2]	anhydrite [$CaSO_4$], hematite [Fe_2O_3]
1050 °C	quartz [SiO_2]	mullite [$Al_6Si_2O_{13}$], hematite [Fe_2O_3], amorphous phase
(d) Lanna ash		
Unheated	anhydrite [$CaSO_4$]	quartz [SiO_2], hematite [Fe_2O_3], diopside [$Ca,Mg(SiO_3)_2$]
900 °C	anhydrite [$CaSO_4$]	quartz [SiO_2], hematite [Fe_2O_3], diopside [$Ca,Mg(SiO_3)_2$]
1050 °C	anhydrite [$CaSO_4$]	quartz [SiO_2], hematite [Fe_2O_3], diopside [$Ca,Mg(SiO_3)_2$]

temperature curve to intersect the temperature axis. It was found that the sinter points of Maemoh ash, Chiengmuan ash and Banpu ash were 650 °C, 750 °C and 770 °C, respectively. It appears that there is an inverse relationship between the sinter point and strength, i.e., ash with lower sinter point gives higher sintered strength, at least for the coal ashes tested. It is also noted that for temperatures lower than 1000 °C there is a

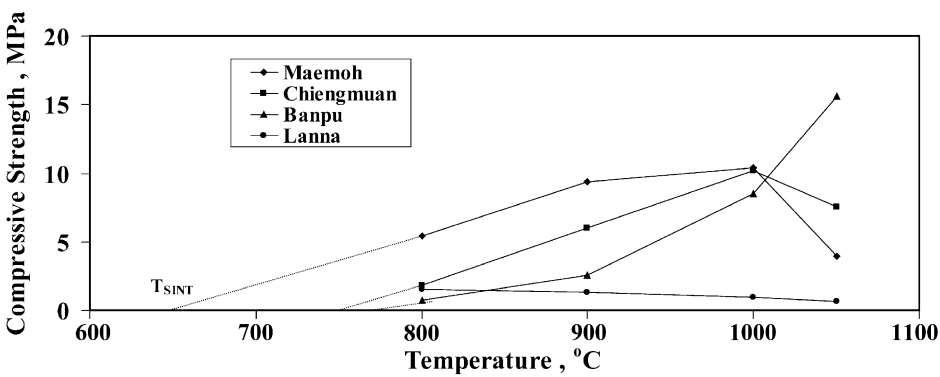

Fig. 1. Compressive strength of sintered coal ashes for temperatures 800–1050 °C.

correlation between strength and amounts of clays (as $\%Al_2O_3$) and anhydrite (as $\%CaO + \%SO_3$) originally containing in the ashes as follows. According to Table 5, Maemoh ash contains relatively high percentage of both clays and anhydrite and thus capable of producing more of low melting eutectics, giving rise to the highest sintered strength (10 MPa at 950 °C). Since XRD results reveal that the crystalline forms of the unheated ashes and the sintered products at 900 °C remain unchanged (Table 4), this low melting eutectics should therefore present in the amorphous phase and could be formed from a reaction between an unstable product of clay transformation and anhydrite during the course of sintering. Chiengmuan ash, which exhibited a lower strength, contains higher clays but lower anhydrite content. Banpu ash has the highest amount of clays but lowest amount of anhydrite, whereas Lanna ash contains lowest amount of clays but highest anhydrite, and both ashes displayed relatively low strength. From this observation, it can be inferred that the magnitude of strength development of an ash sinter is influenced by the relative proportion of clays and anhydrite present in the original ashes, with clays-to-anhydrite percent ratio of approximately 1 giving the highest sintered strength (see Fig. 2).

At the higher temperature range of 1000–1050 °C, the trend of sintered strength of pure ashes is as follows: Banpu > Chiengmuan > Maemoh > Lanna (Fig. 1). This trend is in accord with the amount of clays originally present in the ashes, with ash having higher clays content develops higher strength (see Table 5 at 1050 °C). Therefore, the amount of clays is of prime importance to the sintering behaviour of ash at these high temperatures. It should be noted also that at these high temperatures, chemical reactions between the ash components could occur, resulting in higher strength or lower strength of ash pellets compared to that observed at lower temperatures. For Maemoh ash, XRD results at this high temperature (1050 °C) (Table 4a) indicates the disappearance of anhydrite ($CaSO_4$) and the formation of major crystalline phase of anorthite ($CaAl_2Si_2O_8$). This indicates that anhydrite could decompose and some of the low melting eutectics originally formed at the heat treatment temperature was removed by chemical reaction to form this new high melting crystalline solid phases which retarded the sintering rate, and hence caused a reduction in strength. Sintering behaviour of Chiengmuan ash at this higher temperature range was similar to Maemoh ash (Fig. 1), except that there was a depletion of anhydrite and the formation of new high melting crystalline phase of albite ($NaAlSi_3O_8$) as a minor phase, as shown in Table 4b.

Of all the test ashes, the compressive strength of Banpu ash increased continually with increasing temperature up to the maximum temperature of 1050 °C (Fig. 1). XRD

Table 5
Clays and anhydrite compositions in ASTM ashes

Ash	Clays ($\%Al_2O_3$)	Anhydrite ($\%CaO + \%SO_3$)	Clays/anhydrite % ratio	Strength (MPa) at	
				950 °C	1050 °C
Banpu	29.2	3.5	8.3	5.0	16.0
Chiengmuan	23.1	13.5	1.7	8.0	7.5
Maemoh	18.9	29.7	0.64	10.0	3.5
Lanna	8.1	53.2	0.15	1.0	1.0

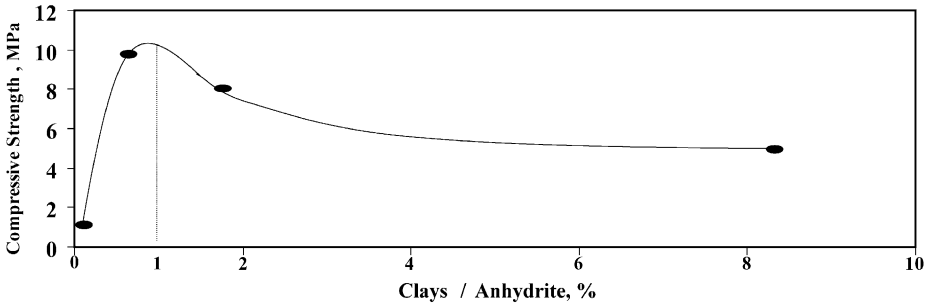

Fig. 2. Variation of ash sinter strength with clays-to-anhydrite percent ratio, at sintering temperature of 950 °C.

result of Banpu ash at this high temperature indicates the disappearance of anhydrite and the formation of mullite ($Al_6Si_2O_{13}$) (Table 4c). However, the formation of mullite should have no direct bearing on the strength reduction like that observed with Maemoh ash and Chiengmuan ash because mullite does not form at the expense of low melting material but it is a high temperature transformation product of kaolinite presenting in the ash. The observed disappearance of anhydrite indicates the possible chemical reaction of anhydrite with other types of clays, which could result in the formation of more liquid glassy phase, thus giving the continued increase in pellet strength due to viscous sintering. The disappearance of anhydrite and the consequent increase of sintered strength was also reported by Jung and Schobert [21] and Benson et al. [27]. In these works, a reaction of anhydrite and clays formed calcium aluminosilicate "glue" or low melting calcium-rich sulfur-poor glass. The presence of this phase increased the rate of viscous flow sintering and led to higher sintered strength.

For Lanna ash, the very low pellet strength (Fig. 1) and the chemically unchanged phase observed with XRD (Table 4d) indicate that the forms of inorganic matter in this type of ash are almost insensitive to change in sintering temperature. The chemical composition of Lanna ash which contains the lowest amounts of clays compared to the other test ashes should be responsible for this kind of low-strength behaviour. As a result, Lanna ash contains less low melting material to initiate sintering and lesser extent of chemical reactions occur between ash components, giving very low strength development. The relationship between associated chemical composition and sintering behaviour of this ash warrants further investigation. Private communication with the Electricity Generating Authority of Thailand (EGAT) revealed that Lanna coal is a good coal for combustion and regularly used to blend with other coals that exhibit ash deposition problems.

3.3. Sintering of coal ashes mixed with bed materials and additives

The results of coal ashes mixed with bed materials (sand, CaO, $CaCO_3$, and $CaSO_4$) and additives (gibbsite and andalusite) are shown in Figs. 3 and 4, respectively. In general, it can be observed that these materials decreased the strength of the test coal ashes, except in the case of Banpu ash with added CaO, $CaCO_3$ and $CaSO_4$, with an

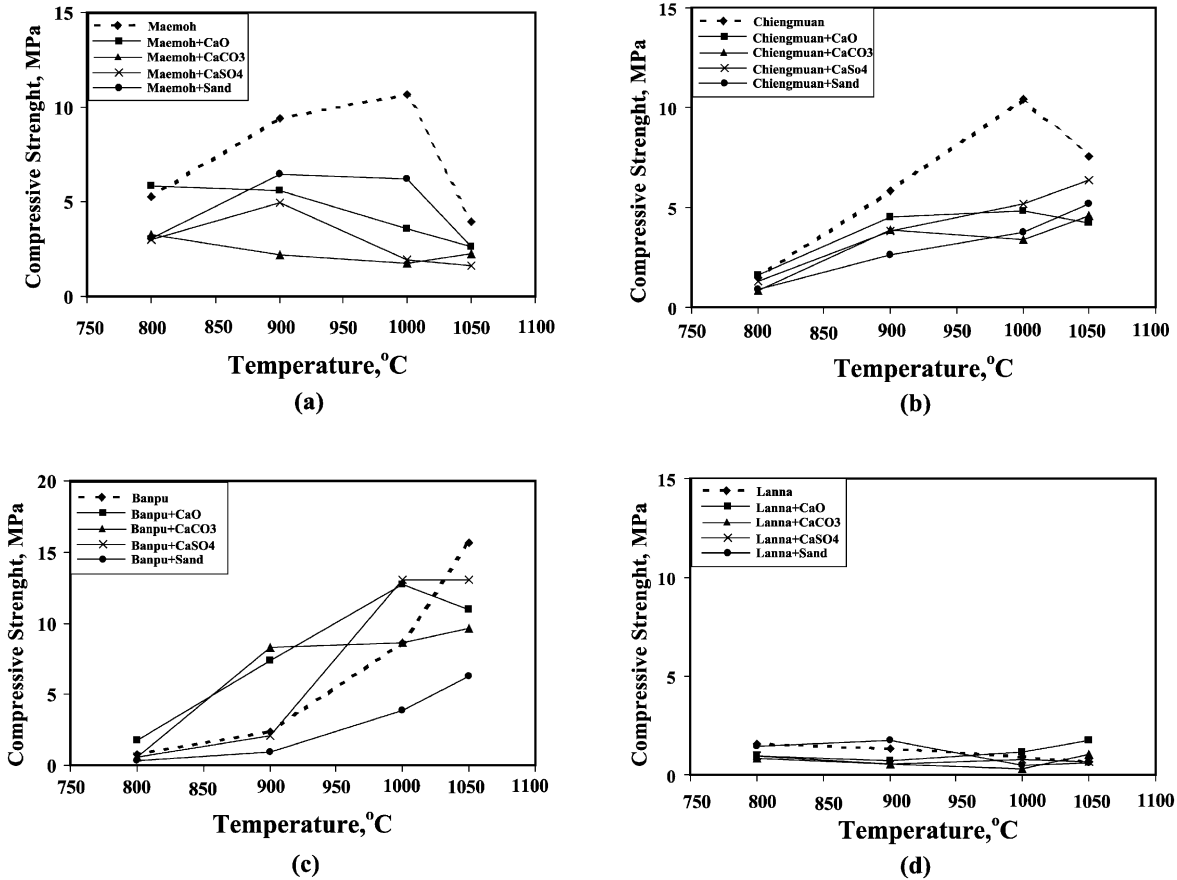

Fig. 3. Compressive strength of sintered ash mixed with 15 wt.% each of CaO, $CaCO_3$, $CaSO_4$ and sand: (a) Maemoh, (b) Chiengmuan, (c) Banpu, (d) Lanna.

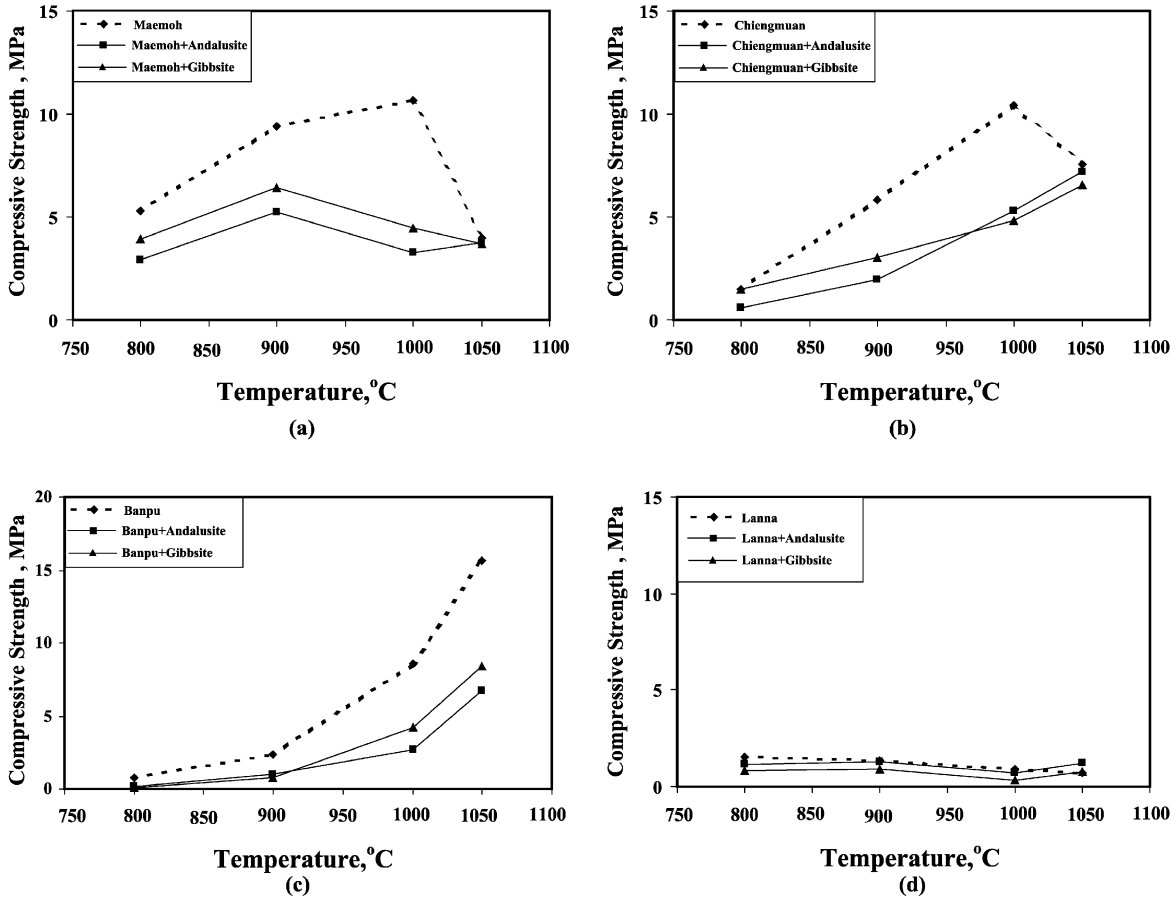

Fig. 4. Compressive strength of sintered ash mixed with 15 wt.% each of andalusite and gibbsite additives: (a) Maemoh, (b) Chiengmuan, (c) Banpu, (d) Lanna.

average reduction of about 50% but again had no significant effect on Lanna ash. XRD results of these samples (Table 6) revealed that sand, $CaSO_4$ and andalusite were still present in the heat-treated pellets. For other materials, CaO remained as amorphous solid, $CaCO_3$ decomposed to amorphous CaO and gibbsite transformed to amorphous alumina (Al_2O_3) but these amorphous phases could not be detected in the XRD diffractograms. In addition, there was neither the disappearance of anhydrite nor the formation of new high melting crystalline materials as occurred in the tests without the

Table 6
XRD analysis of coal ashes mixed with bed materials and additives, sintered at 1050 °C

Ash condition	Major crystalline phases	Minor crystalline phases
Maemoh + $CaCO_3$	anhydrite ($CaSO_4$)	diopside, aluminian [Ca(Mg,Fe,Al)(Si,Al)$_2$ O$_6$], albite, calcian, ordered [(Na,Ca)Al(Si,Al)$_3$ O$_8$], gehlenite (Ca_2 Al_2 Si O_7), hematite (Fe_2O_3), quartz (SiO_2)
Maemoh + CaO	anhydrite ($CaSO_4$)	diopside, aluminian [Ca(Mg,Fe,Al)(Si,Al)$_2$ O$_6$], albite, calcian, ordered [(Na,Ca)Al (Si,Al)$_3$ O$_8$], hematite (Fe_2O_3), quartz (SiO_2)
Maemoh + $CaSO_4$	anhydrite ($CaSO_4$)	diopside, aluminian [Ca(Mg,Fe,Al)(Si,Al)$_2$ O$_6$], albite, calcian, ordered [(Na,Ca)Al (Si,Al)$_3$ O$_8$], hematite (Fe_2O_3), quartz (SiO_2)
Maemoh + sand	quartz (SiO_2)	anhydrite ($CaSO_4$), albite, calcian, ordered [(Na,Ca)Al (Si,Al)$_3$ O$_8$], hematite (Fe_2O_3)
Maemoh + andalusite	anhydrite ($CaSO_4$)	andalusite (Al_2SiO_5), albite, calcian, ordered [(Na,Ca)Al (Si,Al)$_3$ O$_8$], hematite (Fe_2O_3), quartz (SiO_2), diopside [Ca Mg (SiO_3)$_2$]
Maemoh + gibbsite	anhydrite ($CaSO_4$)	albite, calcian, ordered [(Na,Ca)Al (Si,Al)$_3$ O$_8$], hematite (Fe_2O_3), quartz (SiO_2), diopside [Ca Mg (SiO_3)$_2$]
Banpu + $CaCO_3$	quartz (SiO_2)	anhydrite ($CaSO_4$), kyanite (Al_2SiO_5), hematite (Fe_2O_3)
Banpu + CaO	quartz (SiO_2)	anhydrite ($CaSO_4$), kyanite (Al_2SiO_5), hematite (Fe_2O_3)
Banpu + $CaSO_4$	quartz (SiO_2)	anhydrite ($CaSO_4$), kyanite (Al_2SiO_5), hematite (Fe_2O_3)
Banpu + sand	quartz (SiO_2)	anhydrite ($CaSO_4$), hematite (Fe_2O_3)
Banpu + andalusite	quartz (SiO_2)	andalusite (Al_2SiO_5), hematite (Fe_2O_3)
Banpu + gibbsite	quartz (SiO_2)	hematite (Fe_2 O_3), mullite(Al_6 Si_2 O_{13})
Chiengmuan + andalusite	quartz (SiO_2)	andalusite (Al_2SiO_5), albite, calcian, ordered [(Na,Ca)Al (Si,Al)$_3$ O$_8$], hematite (Fe_2O_3)
Chiengmuan + gibbsite	quartz (SiO_2)	anhydrite ($CaSO_4$), hematite (Fe_2O_3), albite, calcian, ordered [(Na,Ca)Al (Si,Al)$_3$ O$_8$], montmorillonite [Al Si_2 O_6 $(OH)_2$]
Lanna + andalusite	anhydrite ($CaSO_4$)	diopside [Ca Mg (SiO_3)$_2$], andalusite (Al_2SiO_5), hematite (Fe_2O_3), quartz (SiO_2)
Lanna + gibbsite	anhydrite ($CaSO_4$)	hematite (Fe_2O_3), diopside [Ca Mg (SiO_3)$_2$], albite, calcian, ordered [(Na,Ca)Al (Si,Al)$_3$ O$_8$], quartz (SiO_2)

added materials. This suggests that each added material presumably lowered the strength of the ash pellets by acting as an *inert diluent*, which was capable of reducing the interacting role of anhydrite and clays in forming the low melting eutectics. Although additives and sand decreased the strength of Banpu ash, other bed materials ($CaCO_3$, CaO, and $CaSO_4$) did not significantly alter the strength. These bed materials could, therefore, interact with the abundant clays available in Banpu ash, leading to the formation of more low melt materials and hence did not act purely as inert diluents.

3.4. Sintering of modified ashes

It has been reported that a major mechanism of agglomerate formation in a fluidized bed results from initial adherence of sticky ash particles followed by secondary ash–bed particles interaction [3–5]. Since the ASTM ashes studied in this work may not contain sufficient amount of amorphous phase to cause significant agglomeration and sintering, high purity amorphous silica was mixed with the original ashes to provide the sticky amorphous-phase environment during ash sintering. This modified ash would allow a clearer study of bed agglomeration as well as the associated effects of added bed materials and additives. It may be argued that the sole addition of amorphous silica to produce silicate glassy matrix may not completely simulate the sticky ash condition, since agglomerates collected from some fluidized bed combustors were found to contain sodium sulfate in solidified melt phase of ash compositions [3,6]. However, the amount of sodium sulfate present in the ashes studied in this work is too low ($< 1\%$ Na_2O) to play a significant role in the bed agglomeration process. The addition of 15 wt.% amorphous silica to the test ashes was considered to give sufficient amorphous phase for examining the possible effects of bed materials and additives on the extent of ash sintering.

The results of compressive strength of the four modified ashes are displayed in Fig. 5. The general observation is that amorphous silica significantly increases the strength of

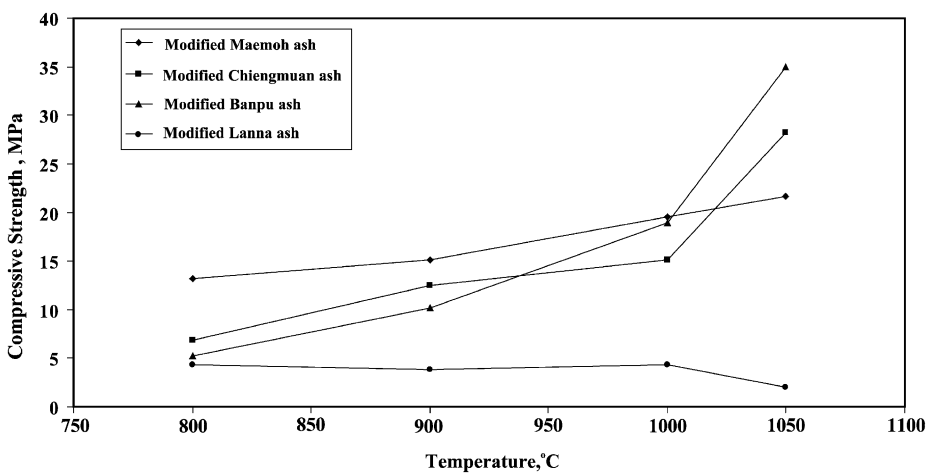

Fig. 5. Compressive strength of sintered modified ashes.

pure coal ashes and the strength tends to increase with temperature for all the ashes tested (see Fig. 1 for comparison). For temperatures below 1000 °C, similar trend of strength–temperature relation is observed as compared to that of pure coal ashes, with modified Maemoh ash showing the highest strength. At temperatures above 1000 °C, modified Banpu ash gave the highest strength, with a maximum strength of 36 MPa being observed at 1050 °C—an increase of almost 120% over that of the pure ash at the same sintering temperature.

XRD results of these sintered modified ashes (Table 7) show somewhat similar mineralogical phases to the pure sintered ashes (Table 4) except that they possessed more of the amorphous phase. This higher amount of amorphous phase as indicated by the occurrence of very broad backgrounds in the XRD diffractogram was attributed to the possible chemical reaction of added amorphous silica with alkali, alkaline earth and iron compounds in the ash components to form low melting silicate glasses. SEM photomicrographs of modified Banpu ash and modified Maemoh ash (Figs. 6a and 7a) confirm the results of strength and XRD analysis, showing a high degree of particle deformation and fusion.

The effect of adding 15 wt.% of bed materials and additives on the strength development of modified Maemoh ash and modified Banpu ash sintered at 1000 °C is illustrated in Fig. 8. According to their roles and effects on the strength behaviour, these materials can be classified into three distinct groups, i.e., Group I ($CaSO_4$, CaO, $CaCO_3$), Group II (sand and andalusite) and Group III (gibbsite). From the results, it is seen that sand and andalusite (Group II) gave intermediate reduction of sintered strength.

Table 7
XRD analysis of sintered pellets of modified ashes sintered at 900 °C and 1050 °C

Ash condition	Major crystalline phases	Minor crystalline phases
Modified Maemoh (900 °C)	anhydrite [$CaSO_4$]	quartz [SiO_2], hematite [Fe_2O_3], amorphous phase
Modified Maemoh (1050 °C)	anorthite [$CaAl_2Si_2O_8$]	diopside [Ca,Mg (SiO_3)$_2$], hematite [Fe_2O_3], quartz [SiO_2], anhydrite [$CaSO_4$], cristobalite [SiO_2], amorphous phase
Modified Banpu (900 °C)	quartz [SiO_2]	anhydrite [$CaSO_4$], hematite [Fe_2O_3], amorphous phase
Modified Banpu (1050 °C)	quartz [SiO_2]	cristobalite [SiO_2], hematite [Fe_2O_3], mullite [Al_6 Si_2O_{13}], amorphous phase
Modified Chiengmuan (900 °C)	quartz [SiO_2]	anhydrite [$CaSO_4$], hematite [Fe_2O_3], nepheline [Na Al SiO_4], amorphous phase
Modifed Chiengmuan (1050 °C)	quartz [SiO_2]	cristobalite [SiO_2], anhydrite [$CaSO_4$], albite [$NaAlSi_3O_8$], hematite [Fe_2O_3], amorphous phase
Modified Lanna (900 °C)	anhydrite [$CaSO_4$]	hematite [Fe_2O_3], diopside [Ca, Mg (SiO_3)$_2$], quartz [SiO_2]
Modified Lanna (1050 °C)	anhydrite [$CaSO_4$]	diopside [Ca, Mg (SiO_3)$_2$], hematite [Fe_2O_3], quartz [SiO_2]

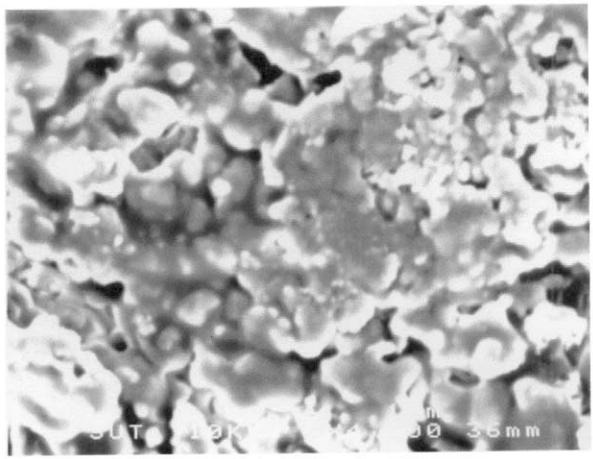

(a)

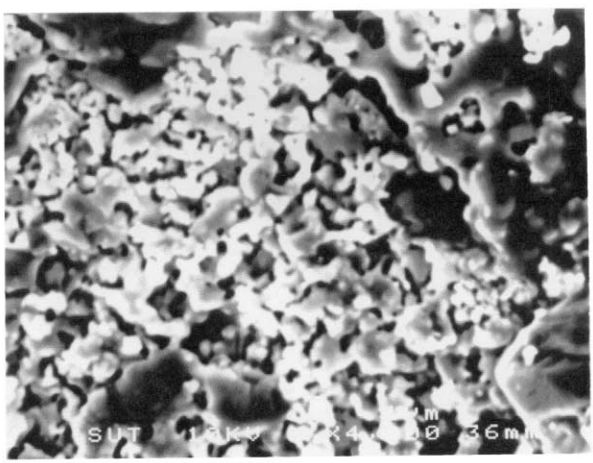

(b)

Fig. 6. SEM photomicrographs of (a) modified Banpu ash, sintered at 1050 °C in air and (b) modified Banpu ash + gibbsite, sintered at 1050 °C in air.

Since both sand and andalusite still remained in crystalline forms after sintering, the possible role of these two materials in the strength reduction would be that they acted simply as *inert diluents.*

Addition of gibbsite (Group III) shows a maximum drop in sintered strength by 52% and 65% for modified Banpu ash and modified Maemoh ash, respectively. Linjewile and Manzoori [6] previously studied the role of gibbsite in controlling the agglomeration of burning low-rank coals in a pilot-scale fluidized bed combustor. They proposed that

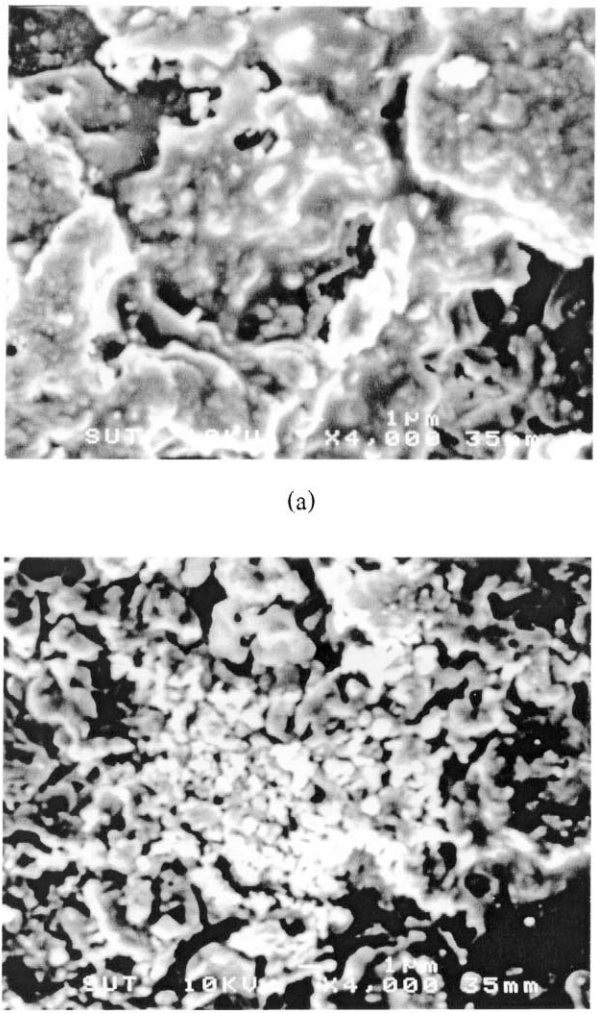

(a)

(b)

Fig. 7. SEM photomicrographs of (a) modified Maemoh ash, sintered at 1050 °C in air and (b) modified Maemoh ash + gibbsite, sintered at 1050 °C in air.

gibbsite, after being transformed to amorphous alumina and with developed internal area of 88 m^2/g, was able to remove molten ash constituents available for strength development by viscous flow sintering. In line with the work of these investigators, it is therefore reasonable to propose that the role of gibbsite in the strength reduction involves the combined effect of inert dilution and molten ash adsorption into the porous solids. This mechanism is referred to as *inert / adsorption effect*. The hypothesis of molten ash removal by gibbsite during sintering was verified by the SEM data and by a simple strength volume calculation as follows. First, Figs. 6 and 7 show SEM photomi-

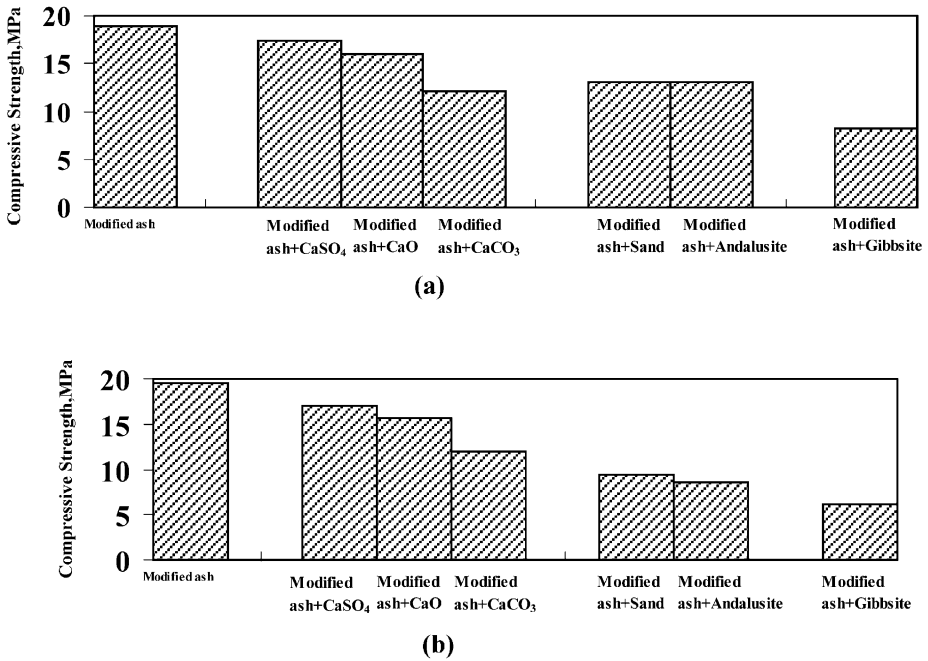

Fig. 8. Effect of bed materials and additives (15 wt.%) on compressive strength of modified ashes, sintered at 1000 °C: (a) Banpu ash, (b) Maemoh ash.

crographs (4000× magnification) of sintered pellets of modified Banpu and modified Maemoh ashes, with and without added gibbsite. It is seen that there is clear evidence of the disappearance of portion of the molten ash, giving a more porous structure of the sintered mass. Second, the porous structure of a sample of gibbsite heat treated at 1050 °C was identified with a surface area analyzer (ASAP 2010, Micromeritics). The results showed that the heat-treated gibbsite, which was transformed into amorphous alumina (Al_2O_3), had the following properties: BET surface area 50 m^2/g, specific total pore volume 0.21 cm^3/g and an average pore size of 25 nm, with most of the pores being in the mesopore range of 5–50 nm. It was proposed previously that the role of gibbsite in lowering the pellet strength was by acting as an inert diluent and by the removal of molten ash into the pores of amorphous alumina. If it is assumed that the lowering of strength by the inert effect of gibbsite is the same as that of sand or andalusite, Fig. 8a shows that the removal of molten ash alone would cause a drop of strength from 13 to 8 MPa, a decrease by 38.46%. Next, it is further assumed that the amount of molten ash removed is proportional to the decrease in pellet strength. Simple calculation shows that the total pore volume of amorphous alumina and total volume of molten ash (assuming to be calcium silicate glass) are 0.0024 and 0.0062 cm^3, respectively. Therefore, the percent removal of molten ash into the pores is found to be 38.71%, which compares very well with the strength reduction of 38.46% as shown previously. Evidence from SEM data and strength–volume calculation suggests that the role of gibbsite in the

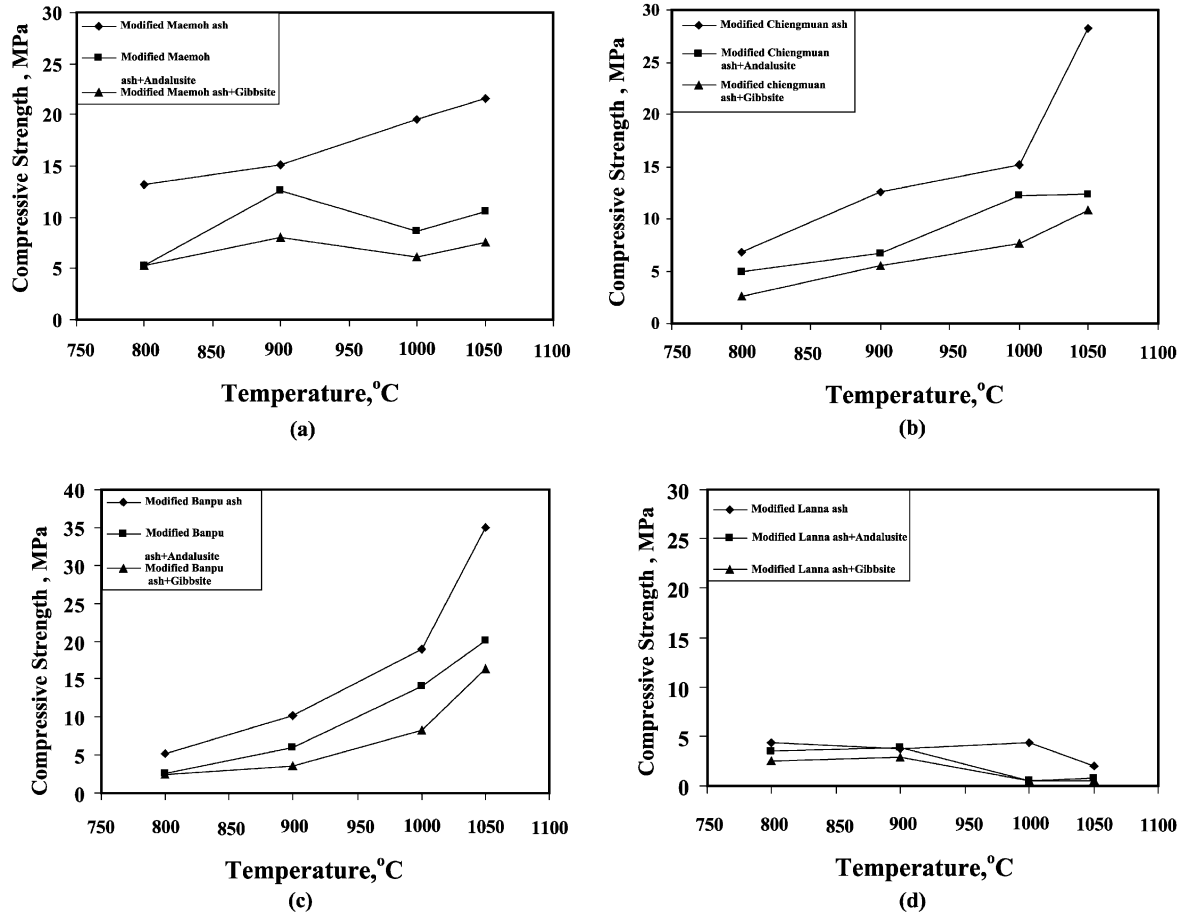

Fig. 9. Effect of temperature and additives on the compressive strength of modified ashes: (a) Maemoh, (b) Chiengmuan, (c) Banpu, (d) Lanna.

strength reduction by molten ash removal is possible due to its porous structure and low viscous nature of molten ash at this high sintering temperature.

Calcium-based bed materials (Group I) gave the lowest strength reduction of sintered pellets. It should be noted that the addition of $CaCO_3$ or CaO should give the same proportional effect on the strength, since $CaCO_3$ can decompose into CaO of lower mass. From Fig. 8a, the strength ratio of $CaCO_3/CaO$ can be estimated to be 0.65 and this number is comparable to the molecular weight ratio $CaO/CaCO_3$ of 0.56, proving no significant difference in the sintering behaviour of these two materials when added to the modified ash. Overall, this group of bed materials could somehow associate with added amorphous silica to form additional low melting amorphous phase that helped increase the sintering rate. The net result was that the pellet strength could be maintained closer to that of the original modified ashes. These materials therefore affected the sintered strength by a combined *inert / reaction effect*.

Fig. 9 shows specifically the effects of temperature and additives on the compressive strength of modified ashes. It is clear that additives were able to lower the pellet strength at all temperatures. For each modified ash it appears that gibbsite is more effective than andalusite in lowering the strength, particularly at temperatures above 900 °C. Again the modified Lanna ash seems to be insensitive to the presence of both types of additives. It is clear that the use of a modified ash in studying fluidized-bed agglomeration proposed in this work is a useful approach in identifying the role and effect of various bed materials and additives.

It should be emphasized that the role of SO_2 on the sintering behaviour was not investigated in this work, although in a fluidized-bed operation, the presence of SO_2 can enhance the rate of sintering through sulfation of the calcium-rich species [10,21,27]. Therefore, the strength development of sintered pellet observed in this study was due predominantly to the sintering of silicates. The significance of silicates phase on sintering rate can be comprehended from test results of Lanna ash. This ash contains very low contents of clays and silica and thus exhibited almost no strength development under varying temperatures. However, Lanna ash contains high percentage of CaO and it might be worthwhile to investigate further the sintering of this ash under SO_2 environment.

4. Conclusions

Bed agglomeration and sintering in fluidized bed combustion and the role of additives (andalusite and gibbsite) and bed materials (sand, $CaCO_3$, CaO, and $CaSO_4$) were investigated by following the compressive strength of ash sinters as a function of temperature (800–1050 °C). Lanna ash did not develop any appreciable strength, and it was not influenced by changes in sintering temperature and the association of any added materials, presumably due to its very low clays and silica content. The strength–temperature curves of the remaining coal ashes (Maemoh, Banpu and Chiengmuan) showed a definite difference for temperatures below and above 1000 °C. This difference was attributed to the role and relative amounts of clays and anhydrite components and the low-melting eutectics in the test ashes. From these results, if the bed temperature is at

the normal operating temperature of a fluidized bed combustor, say 950 °C, Maemoh ash should pose the highest tendency for bed agglomeration and deposit formation problems. However, at higher temperatures (> 950 °C), which could result from ineffective bed mixing, Banpu ash should give the greatest tendency for bed agglomeration.

When bed materials (sand, $CaCO_3$, CaO, and $CaSO_4$) and additives (andalusite and gibbsite) were combined with the ashes, these materials appeared to lower the strength of ash sinters equally, with an average reduction of about 50%. These added materials were believed to lower the strength by acting as inert diluents that prevented the association of clays and anhydrite to form the low melting eutectics.

A condition of sticky sintered ash was purposely formed upon sintering by adding amorphous silica into the test ashes to produce extra low-melting silicate glasses. An increase in sintered strength was clearly indicated at all temperatures for these ashes with a maximum increase of about 120%. When these modified ashes were mixed with bed materials and additives, a reduction in sintered strength was noted and can be explained by three different mechanisms based on three groups of added materials. They are Group I materials ($CaCO_3$, CaO, and $CaSO_4$), giving *inert / reaction effect*; Group II materials (sand and andalusite additive), showing *pure inert effect*; and Group III materials (gibbsite additive), indicating *inert / adsorption effect*. In terms of strength reduction, gibbsite additive appeared to be more effective than andalusite, especially at temperatures above 900 °C.

Acknowledgements

The authors gratefully acknowledge the financial support for this research from Suranaree University of Technology. Part of laboratory work was performed by Miss Naparat Jivaluk and is particularly acknowledged. The coal samples provided by the Electricity Generating Authority of Thailand is highly appreciated.

References

[1] A.R. Manzoori, Fuel 73 (4) (1994) 563.
[2] M.R. Dawson, R.C. Brown, Fuel 71 (1992) 585–592.
[3] S.P. Bhattacharya, A. Kosminski, H. Yan, H.B. Vuthaluru, Combustion of Victorian and South Australian low-rank coals in a circulating fluidized bed combustion pilot plant. The Ninth Japan/Australian Joint Technical Meeting on Coal, Melbourne, June 1–2, 1999.
[4] R.C. Brown, M.R. Dawson, J.L. Smeenk, Bed material agglomeration during fluidized bed combustion, Final Report to the US Department of Energy (DOE), DE96007754XPS, 1996.
[5] B.-M. Steenari, O. Lindqvist, V. Langev, Fuel 77 (5) (1998) 407–417.
[6] T.M. Linjewile, A.R. Manzoori, Role of additives in controlling agglomeration and defluidization during fluidized bed combustion of high-sodium, high-sulphur low-rank coal. Engineering Foundation Conference, Hawaii, 2–7 November, 1997.
[7] H.B. Vulthaluru, D. Zhang, Fuel Process. Technol. 60 (1999) 145–156.
[8] H.B. Vulthaluru, T.M. Linjewile, D. Zhang, A.R. Manzoori, Fuel 78 (1999) 419–425.
[9] B.-J. Skrifvars, M. Hupa, Ind. Eng. Chem. Res. 31 (1992) 1026–1030.
[10] B.-J. Skrifvars, M. Hupa, R. Backman, M. Hiltunen, Fuel 73 (2) (1994) 171–176.

[11] M. Tangsathitkulchai, PhD Dissertation, The Pennsylvania State University, PA, USA, 1986.
[12] H.H. Schobert, R.E. Conn, B. Jung, J. Proc. 4th Annual Pittsburgh Coal Conference, 1987, p. 423.
[13] B.-J. Skrifvars, R. Backman, M. Hupa, G. Sfiris, T. Abyhammar, A. Lyngfelt, Fuel 77 (1/2) (1998) 65–70.
[14] E. Raask, Am. Chem. Soc. Div. Fuel Chem., Preprints 27 (1982) 145.
[15] W.T. Reid, Prog. Energy Combust. Sci. 10 (1984) 159.
[16] B.C. Young, B.G. Miller, D.P. McColler, K.D. Schnabel, D.R. Kleesattei, M.L. Jones, Fundamental combustion and ash fouling, DOE/FF60181-2126, US Department of Energy, Washington, DC, 1986.
[17] B. Jung, H.H. Schobert, Energy Fuels 6 (1992) 59–68.
[18] R.E. Conn, MS Thesis, The Pennsylvania State University, PA, USA, 1984.
[19] M. Tangsathitkulchat, L.G. Austin, Fuel 64 (1985) 86–92.
[20] M. Hupa, B.-J. Skrifvars, A. Moianen, J. Inst. Energy 62 (1989) 131–137.
[21] B. Jung, H.H. Schobert, Energy Fuels 5 (1991) 555–561.
[22] C. Tangsathitkulchai, M. Tangsathitkulchai, Effect of environment atmosphere on the sintering of Thai lignite fly ashes. Proceedings of an Engineering Foundation Conference on Application of Advanced Technology to Ash-Related Problems in Boilers, New Hampshire, USA, Jul. 16–21, 1995, pp. 425–435.
[23] J.W. Nowok, S.A. Benson, M.L. Jones, D.P. Kalmanovich, Fuel 69 (1990) 1020–1028.
[24] J.P. Hurley, J.W. Nowok, J.A. Bieber, B.A. Dockter, Prog. Energy Combust. Sci. 24 (1998) 513–521.
[25] D.H. Barnhart, P.C. Williams, Trans. AIME 78 (1956) 1229.
[26] American Society for Testing and Materials, Annual Book of ASTM Standards, vol. 0505, ASTM, Philadelphia, 1990.
[27] S.A. Benson, F.R. Karner, G.M. Goblirsch, D.W. Brekke, Am. Chem. Soc. Div. Fuel Chem., Preprinted Paper 27 (1) (1982) 174.